

Hedgehog Signaling Components Are Expressed in Choroidal Neovascularization in Laser-induced Retinal Lesion

Katsunori Nochioka¹, Hiroaki Okuda², Kouko Tatsumi², Shoko Morita², Nahoko Ogata¹ and Akio Wanaka²

¹Department of Ophthalmology, Nara Medical University Faculty of Medicine and ²Department of Anatomy and Neuroscience, Nara Medical University Faculty of Medicine, Nara, Japan

Received November 11, 2015; accepted February 22, 2016; published online April 9, 2016

Choroidal neovascularization is one of the major pathological changes in age-related macular degeneration, which causes devastating blindness in the elderly population. The molecular mechanism of choroidal neovascularization has been under extensive investigation, but is still an open question. We focused on sonic hedgehog signaling, which is implicated in angiogenesis in various organs. Laser-induced injuries to the mouse retina were made to cause choroidal neovascularization. We examined gene expression of sonic hedgehog, its receptors (patched1, smoothed, cell adhesion molecule down-regulated by oncogenes (Cdon) and biregional Cdon-binding protein (Boc)) and downstream transcription factors (Gli1-3) using real-time RT-PCR. At seven days after injury, mRNAs for Patched1 and Gli1 were upregulated in response to injury, but displayed no upregulation in control retinas. Immunohistochemistry revealed that Patched1 and Gli1 proteins were localized to CD31-positive endothelial cells that cluster between the wounded retina and the pigment epithelium layer. Treatment with the hedgehog signaling inhibitor cyclopamine did not significantly decrease the size of the neovascularization areas, but the hedgehog agonist purmorphamine made the areas significantly larger than those in untreated retina. These results suggest that the hedgehog-signaling cascade may be a therapeutic target for age-related macular degeneration.

Key words: sonic hedgehog, retina, mouse, choroidal neovascularization

I. Introduction

Age-related macular degeneration (AMD) is a devastating disease that causes blindness in the elderly population, especially in developed countries. AMD is a complex multifactorial disease that involves environmental factors such as cigarette smoking and lifetime sunlight exposure, and genetic components such as factors in the complement system [6, 22, 28]. The multifactorial nature of AMD makes the development of a complete therapy almost impossible [6].

Choroidal neovascularization (CNV) is one of the major pathological changes in AMD and has therefore become a target of therapeutic strategies [6, 10]. Inappropriate angiogenesis causes CNV in the AMD retina. Indeed, several angiogenic factors have been so far implicated in the pathogenesis of CNV. Vascular endothelial growth factor (VEGF)-A, VEGF-B, Angiopoietin1 and Angiopoietin2 are representative angiogenic factors and their pathogenic roles in AMD have been explored [5, 26]. Among these, the angiogenic effect of VEGF-A in CNV has since been established and VEGF-A is currently the best target of anti-AMD therapy; anti-VEGF-A monoclonal antibodies (bevacizumab, ranibizumab) effectively reduce CNV development in AMD patients [23, 44]. Compatible with these studies, blocking of VEGF receptor function is also effective in treating CNV [18, 25]. Although the anti-

Correspondence to: Akio Wanaka, M.D., Ph.D., Department of Anatomy and Neuroscience, Nara Medical University Faculty of Medicine, 840 Shijo-cho, Kashihara City, Nara 634–8521, Japan.
E-mail: akiow@naramed-u.ac.jp

VEGF and anti-VEGF receptor therapies are successful in reducing CNV, their effects are clinically modest and other VEGF-related drugs are also under investigation [46]. Different kinds of anti-angiogenic factor therapies have also been sought to provide more effective treatments. Notch signaling [1] and the Wnt pathway [47] exemplify potential targets for such alternative therapeutic developments.

Sonic hedgehog (Shh) is a powerful angiogenic factor during development [33, 34, 38] and in cancer tissues [37]. The Shh pathway is also implicated in CNV, and because its inhibition reduces CNV [42] the Shh pathway is a candidate target of anti-AMD therapy. Interestingly, a recent genome-wide association study revealed a potential, albeit not significant, association of the Shh pathway components *Gli2* and *Gli3* with AMD [17]. Given the genome association results, we first examined whether Shh signaling components are upregulated in the mouse CNV model. We also investigated whether pharmacological stimulation or inhibition of Shh signaling affects CNV.

II. Materials and Methods

Animals

Adult male C56BL/6 mice (8–10 weeks old, Japan Charles River Laboratory, Yokohama, Japan) were housed in plastic cages under standard laboratory conditions (23±1°C, 55±5% humidity in a room with a 12-hr light-dark cycle) and had access to tap water and food *ad libitum*. The Animal Care Committee of Nara Medical University approved the protocols for this study in accordance with the policies established in the NIH Guide for the Care and Use of Laboratory Animals.

Laser-induced retinal lesions and drug delivery

Adult mice were anesthetized with an intraperitoneal injection of chloral hydrate (Aldrich, TX, USA). The pupils of all animals were dilated using topical 0.5% tropicamide and 0.5% phenylephrine (Midorin P, Santen Pharmaceuticals, Osaka, Japan). We placed a cover glass on the cornea and delivered four laser burns to the retina of one eye at a distance of one to two disc diameters from the optic disc using the krypton laser system (530.9 nm wavelength, MC-7000, NIDEK, Aichi, Japan). Laser settings were 100 mW power and 800 ms duration. We reproducibly generated laser burns 100 µm in diameter without any major damage to retinal arteries or veins. In each mouse, one eye was laser-treated and the other (control) was sham-operated (a cover glass was placed on the cornea but no laser burns were delivered). For mRNA quantification, mice were kept for five or seven days after treatment and then sacrificed by decapitation under deep anesthesia. The eyeballs were enucleated and the retinas were dissected out for real-time PCR analyses (see below). For double-labeling immunohistochemistry, mice were perfused with 4% paraformaldehyde in phosphate buffer at five or seven days after treatment. The retinas were dissected out and 20 µm retinal

sections were cut on a cryostat. The sections were subjected to double-labeling immunohistochemistry (see below). For Shh signaling modification by pharmacological agents, mice were divided into three groups (n=5 for each group) after the laser irradiation. One group received daily intraperitoneal injections of 10 mg/kg cyclopamine (a sonic hedgehog antagonist; Cosmo Bio, Tokyo, Japan) and a second group received daily intraperitoneal injections of 15 mg/kg pumorphamine (a sonic hedgehog agonist; Santa Cruz Biotechnology, TX, USA). The third (control) group received daily injections of vehicle (10% dimethyl sulfoxide in distilled water) alone. At seven days after laser irradiation, all the mice were perfused with 4% paraformaldehyde in phosphate buffer and eyeballs were enucleated. The retinas were subjected to flat-mount immunohistochemistry for CD31 (see below).

Real-time reverse transcriptase-polymerase chain reaction

Total RNA of the retina was extracted using TRIzol (Invitrogen, CA, USA). The extracts were reverse-transcribed using random primers and a QuantiTect Reverse Transcription kit (QIAGEN, Tokyo, Japan), according to the manufacturer's instructions. Real-time RT-PCR was performed using a LightCycler Quick System 350S (Roche Diagnostics, Tokyo, Japan), with SybrGreen Realtime PCR Master Mix Plus (Toyobo, Osaka, Japan). The specific primers used in the present study are listed in Table 1.

Double-labeling immunohistochemistry

Immunohistochemical procedures were described previously [32, 43]. Briefly, the retinal sections were incubated with two primary antibodies in phosphate buffered saline (PBS): one was Armenian hamster anti-CD31 IgG (Developmental Studies Hybridoma Bank, DSHB, clone 2H8; dilution 1:20) and the other was rabbit polyclonal IgG against either Sonic hedgehog (Sigma-Aldrich Japan, AV44235; dilution 1:300), Patched1 (Sigma-Aldrich Japan, SAB4502472; dilution 1:200) or *Gli1* (Abcam Japan, ab92611; dilution 1:400). After being washed with PBS, the sections were incubated with two secondary antibodies in PBS for 2 hr: Alexa 488-conjugated goat IgG against rabbit IgG (Jackson ImmunoResearch; dilution 1:400) and Alexa 594-conjugated goat IgG against Armenian hamster IgG (Jackson ImmunoResearch; dilution 1:400). The labeled sections were counterstained with 4',6-diamidino-2-phenylindole (DAPI, Sigma-Aldrich Japan, D9542) and mounted on glass slides, and coverslips were sealed with Vectashield (Vector Laboratories, CA, USA). We observed the sections using a laser-scanning confocal microscope (Fluoview 1000, Olympus, Tokyo, Japan). For the control experiments of immunohistochemistry, we replaced the primary antibodies (see above) with either Armenian Hamster isotype-control IgG (MBL, Japan, M199-3; dilution 1:20) or rabbit polyclonal isotype-control IgG (Abcam, Japan, ab27472; dilution 1:200) and then treated sections with

Table 1. Forward and reverse primers employed in the present study. Abbreviated and full names of each gene and NCBI reference numbers are indicated.

Official Symbol	Forward primer	Reverse primer	NCBI Reference	Gene name
Shh	CAAGAACTCCGAACGATTTAAGG	GCATTTAACTTGTCTTTGCACC	NM_009170.3	sonic hedgehog
Ihh	GTGCATTGCTCTGTCAAGTCTG	GGTCTCTGGCTTTACAGCTG	NM_010544.2	Indian hedgehog
Dhh	TCCACGTATCGGTCAAAGCTGA	CCAGTCACCACGATGTAGTTCC	NM_007857.4	desert hedgehog
Ptch1	CAGCTAATCTCGAGACCAACGTG	GAGTCTGTATCATGAGTTGAGG	NM_008957.2	patched homolog 1
Smo	GACATGCACAGCTACATCGCAG	CGCAGGGTAGCGATTGGAGTTCC	NM_176996.4	smoothed homolog (Drosophila)
Gas1	TCAACGACTGCGTGTGCGATGG	GGACCGTTGCTCGCATCTGG	NM_008086.2	growth arrest specific 1
Cdon	CCAGTGCGTTGCCAACAAACAGC	TGGTACCCTGCAGCCAATGAAGC	NM_021339.2	cell adhesion molecule-related/down-regulated by oncogenes
Boc	TACTACTGCTTTGGATTCTCATGG	AGTCACGTTCCATCCATGGTGGCTC	NM_172506.2	biregional Cdon binding protein
Gli1	ATAGTGAGCCATGCTGTCTCC	TCTCTCTGGCTGCTCCATAACC	NM_010296.2	GLI-Kruppel family member GLI1
Gli2	TACCACCAGATGACCTCATGG	CGTGGACTAGAGAATCGTGATGC	NM_001081125.1	GLI-Kruppel family member GLI2
Gli3	GAGAACAGATGCAGCGAGAAGG	TGAGACCTGCACACTCTGAGG	NM_008130.2	GLI-Kruppel family member GLI3
Vegfa	CCTGGCTTTACTGCTGTACTCTCC	AGCTTCGCTGGTAGACATCCATG	NM_001025250.3	vascular endothelial growth factor A
Vegfb	AGCTGTGTGACTGTGCAGCGCTG	CATTGGCTGTGTTCTCCAGG	NM_011697.3	vascular endothelial growth factor B
Flt1	CCAGCATGTCATGAAGCAGG	GTC AAGGTGCTGCAGAATTGC	NM_010228.3	FMS-like tyrosine kinase 1
Flk1 (Kdr)	GGAGCCTACAAGTCTCGTACC	GTTCTCGGTGATGTACACGATGC	NM_010612.2	kinase insert domain protein receptor
Angpt1	TCAGCACTGGAGCATGTGATGG	TCAAGCATGGTGGCCGTGTGG	NM_009640.4	angiopoietin 1
Angpt2	TCTACCTCGTGGTGAAGAGTCC	TGCAGATGCATTGTCAATTGTC	NM_007426.4	angiopoietin 2
Tie1	GTGTCTGTATGACCATGATGG	AGACCTTACAACCTGCTGTGCC	NM_011587.2	tyrosine kinase with immunoglobulin-like and EGF-like domains 1
Tie2 (Tek)	GAGGAAACCTGTTCACTCAGC	ATGGCAGACTCCATTGTTCTTGC	NM_013690.3	endothelial-specific receptor tyrosine kinase
Gfap	TGGAGAGGGACAACCTTGCACAGG	CTTCATCTGCCTCCTGTCTATACG	NM_001131020.1	glial fibrillary acidic protein
Cxcr4	ATGGAACCGATCAGTGTGAGTATA	AGATGATGAAGTAGATGGTGGG	NM_009911.3	chemokine (C-X-C motif) receptor 4
Hif1a	AAGCTTCTGTTATGAGGCTCACC	CACCATCACAAAGCCATCTAGG	NM_010431.2	hypoxia inducible factor 1, alpha subunit

corresponding anti-Hamster or anti-rabbit secondary antibodies, respectively. We also checked whether or not there were cross-reactions between the primary antibodies (Armenian hamster or rabbit) and the different species-specific secondary antibody (anti-rabbit or anti-Armenian hamster ones, respectively) by incubating sections with these combinations of antibodies. We observed these control sections under a laser-scanning confocal microscope.

Quantification of CNV area using CD31 immunohistochemistry

The isolated retina was subjected to CD31 immunohistochemistry; briefly, the retina was incubated overnight with anti-CD31 antibody (see above) and then treated with secondary Alexa-488-conjugated anti-hamster IgG antibody (Jackson ImmunoResearch; dilution 1:400). The immunolabeled retina was cut radially at four angles (0, 90, 180 and 270°) and then flat-mounted on a glass slide. The retina was observed under a laser-scanning confocal microscope (Fluoview 1000, Olympus). Because CD31 is expressed in the endothelial cells, CD31 immunohistochemistry could clearly reveal the choroidal neovascularization with proliferated endothelial cells (Fig. 4). Using ImageJ software (NIH, USA), we measured CD31-positive areas and subjected them to statistical analyses.

Statistical analysis

Graphical data are presented as the mean±SEM. Sta-

tistical analyses of the results of real-time RT-PCR were performed using the unpaired Student's *t*-test. Morphometric data of choroidal neovascularization were subjected to Bonferroni-Holm adjustment for multiple comparisons. Differences were considered significant when the *p* value was <0.05.

III. Results and Discussion

We first examined whether our laser delivery system efficiently and accurately rendered CNV in the retina by checking the time-course of expression of injury- and angiogenesis-related factors using real-time RT-PCR. As injury-related factors, we chose glial fibrillary acidic protein (GFAP; Müller glial marker), Cxcr4 (chemokine) and Hif1a (tissue hypoxia-related factor). Figure 1A indicates that all three factors were significantly upregulated at day 7 after laser treatment. GFAP [11], Cxcr4 [29, 40] have been reported to be upregulated in CNV lesions in animal models, and Hif1a [41, 45] in both an animal model and human AMD. The present results confirm that our laser-induced CNV at 7 days after treatment is a valid model of this aspect of AMD. Angiogenic factors such as VEGF and angiopoietins are expressed in the AMD retina, and anti-VEGF treatment has successfully reduced CNV formation [9, 15, 23]. Figure 1B shows the expression patterns of mRNAs for eight angiogenesis-related factors; at 7 days after laser delivery, five of these mRNAs (VEGF-A, Flt1,

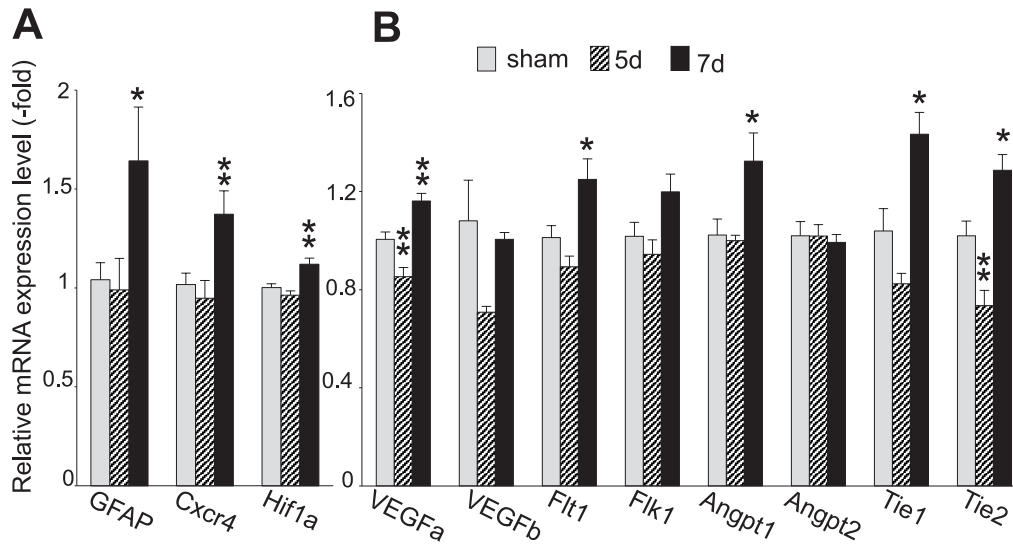


Fig. 1. Injury- and angiogenesis-related genes are upregulated in laser-induced retinal lesions. **A:** GFAP, Cxcr4 and Hif1a gene expression in sham-operated retinas and in retinas at 5 or 7 days after laser treatment was examined by real-time RT-PCR. Values are expressed as ratios to those of control (sham-operated) retinas. A single asterisk indicates $p < 0.05$ vs. the sham group and double-asterisk indicates $p < 0.01$ vs. the sham group ($n=3$). **B:** Expression of angiogenesis-related genes (VEGFa, VEGFb, Flt1, Flk1, Angiopoietin1, Angiopoietin2, Tie1 and Tie2) was examined using real-time RT-PCR in sham-operated retinas and in retinas at 5 or 7 days after laser treatment. Values are expressed as ratios to those of control (sham-operated) retinas. Asterisk indicates $p < 0.05$ vs. sham group and double-asterisk indicates $p < 0.01$ vs. sham group ($n=3$).

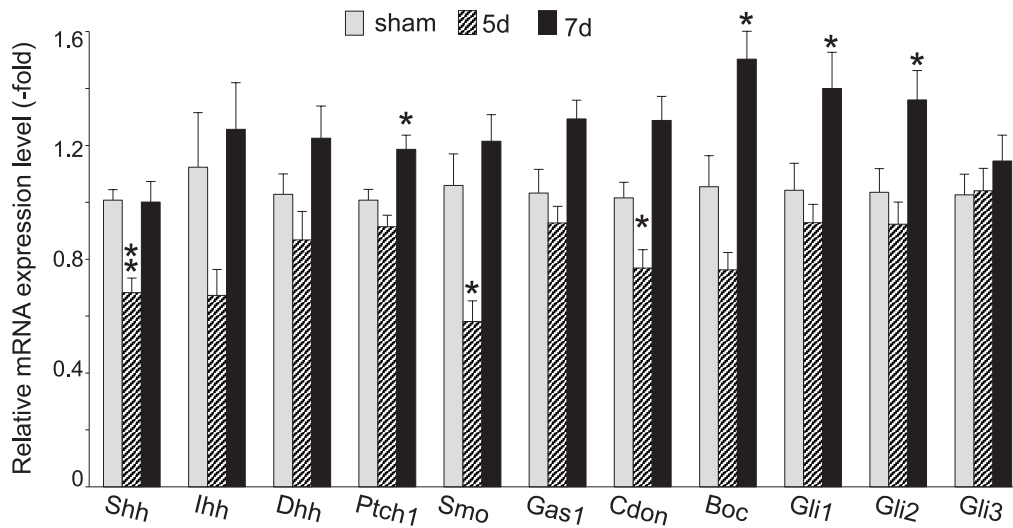


Fig. 2. Laser-induced retinal lesions show upregulation of genes involved in the hedgehog signaling pathway. Sham-operated retinas, and retinas at 5 and 7 days after laser treatment, were isolated and the expression of hedgehog signaling component genes was examined by real-time RT-PCR. Values are expressed as ratios to those of control (sham-operated) retinas. At 7 days after laser treatment, Ptch1, Cdon, Boc, Gli1 and Gli2 mRNAs were significantly upregulated. Asterisk indicates $p < 0.05$ vs sham group and double-asterisk indicates $p < 0.01$ vs sham group. Ihh: Indian hedgehog, Dhh: Desert hedgehog, Ptch1: patched 1, Smo: smoothed, Gas1: growth arrest specific gene 1, Cdon: cell adhesion molecule down-regulated by oncogenes, Boc: biregional Cdon-binding protein.

angiopoietin 1, Tie1 and Tie2) were upregulated. These results demonstrate that our laser-induced CNV method is comparable to those in previous studies and should therefore be applicable to assessing the contribution of the Shh signaling pathway.

We next examined temporal expression patterns of Shh signaling components in retinas with laser-induced CNVs. Hedgehog ligands include Shh, Indian hedgehog (Ihh) and Desert hedgehog (Dhh), all of which share com-

mon signaling components (i.e., receptors and intracellular signaling molecules) [8, 27], and there are two canonical receptors, patched (Ptch) and smoothed (Smo). In addition to these, cell adhesion molecule down-regulated by oncogenes (Cdon) and biregional Cdon-binding protein (Boc) are recently identified receptors for hedgehog [36]. Growth arrest specific gene 1 (Gas1), a transmembrane protein, modulates hedgehog signaling [21, 24, 31]. We also examined the expression patterns of the Gli family of

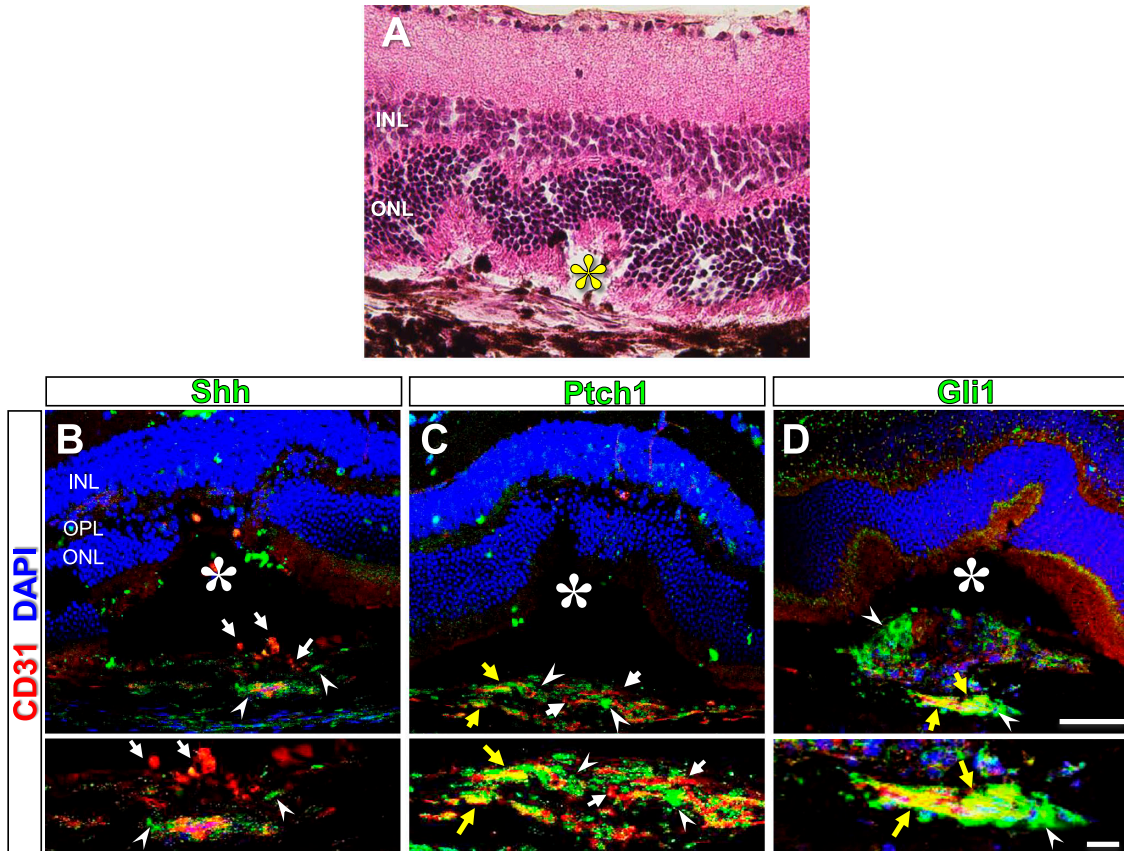


Fig. 3. Double-labeling of Shh signaling components and CD31 in the injured retina. **A:** A laser-induced retinal lesion (7 days after laser treatment) was sectioned on a cryostat and stained with hematoxylin and eosin, showing general histological features of a lesion. The asterisks in **A–D** indicate space between the injured retina and the pigment epithelium. INL, inner nuclear layer; ONL, outer nuclear layer. **B:** Shh (green) and CD31 (red) double-labeled section. Arrows indicate CD31-positive endothelial cells (red) that proliferated in response to injury. Arrowheads show Shh immunoreactivity (green). The lower image shows a higher-magnification view of neovascularization. Bar=100 μ m (also for **B** and **C**). INL, inner nuclear layer; OPL, outer plexiform layer; ONL, outer nuclear layer. **C:** Ptch1 (green) and CD31 (red) double-labeled section. White arrows indicate CD31-positive endothelial cells and white arrowheads indicate Ptch1-positive structures. Yellow arrows indicate CD31-positive endothelial cells with Ptch1 immunoreactivity. **D:** Gli1 immunoreactivity is shown in green. White arrowheads indicate Gli1 immunoreactivity and yellow arrows indicate Gli1 and CD31 double-positive cells.

intracellular signaling molecules. The Gli family consists of three members, Gli1, 2 and 3, which translocate into nucleus upon activation of cell-surface receptors. Gli family members are zinc-finger proteins that function as transcription factors [19]. Figure 2 shows the temporal expression patterns of the above-mentioned hedgehog signaling components. Consistent with the GFAP, Cxcr4 and Hif1 expression patterns, those of the hedgehog signaling components tended to increase at 7 days after laser treatment. Among the factors, Ptch1 and Boc mRNAs were significantly upregulated in treated compared to sham-operated retinas, and Gli1 and Gli2 were also induced at 7 days after laser treatment. It should be noted that mRNA levels of the hedgehog ligands Shh, Ihh and Dhh were comparable to their sham-operated control levels at 7 days after laser treatment. These results indicate that the laser-treated retinas with CNV lesions are capable of responding to hedgehog ligands, although the ligands themselves are not upregulated in the lesions. In the context of the development of CNV lesions and their progression, the cellular

localization of the upregulated components of the hedgehog-signaling pathway is of particular interest. We therefore next examined the localization of signaling components with immunohistochemistry.

We examined the cellular localization patterns of hedgehog signaling components with special reference to endothelial cells forming CNV lesions. We confirmed that immunohistochemistry with non-specific IgGs of either Armenian hamster or rabbit did not produce any signals and that there were no cross-reactions between primary Armenian hamster IgG and secondary anti-rabbit IgG or between primary rabbit IgG and secondary anti-Armenian hamster IgG (data not shown). Figure 3 shows laser-photocoagulated retinal sections that were stained with hematoxylin and eosin (**A**) and that were double-labeled with anti-CD31 antibody (a marker for endothelial cells) and with antibodies for Shh (**B**), Ptch1 (**C**) and Gli1 (**D**). CD31-positive cells formed a cluster just beneath the neural retina in the laser-induced lesion. Ptch1 immunoreactivity co-localized with the CD31-positive cell cluster (Fig. 3C).

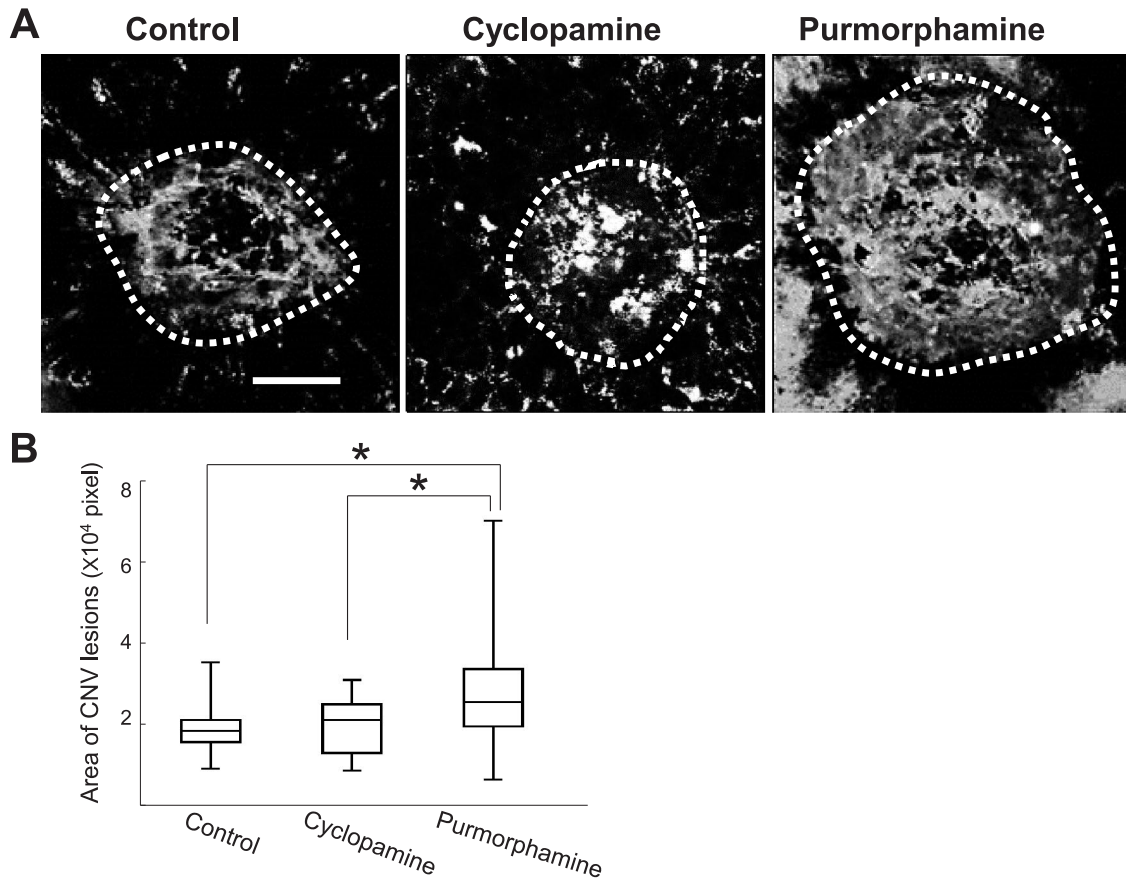


Fig. 4. Effects of Shh agonist and antagonist on laser-induced CNV lesions. **A:** Representative pictures of control (vehicle-treated), cyclopamine-treated and purmorphamine-treated CNV lesions stained with anti-CD31 antibody. Dotted lines demarcate the edges of the CNV areas. Bar=200 μ m. **B:** The areas of CNV lesions (four CNV lesions per eye, three mice per group, n=12 per group) were measured with ImageJ software and statistically analyzed for control (vehicle-treated), cyclopamine-treated and purmorphamine-treated groups. Purmorphamine-treated CNV lesions are significantly (* indicates $p < 0.05$) larger than cyclopamine-treated and control CNV lesions.

Gli1 immunoreactivity also localized to the CD31-positive cell cluster (Fig. 3D). In the control sham-operated retina, we observed neither Ptch1 nor Gli1 immunoreactivities (data not shown). Consistent with the real-time RT-PCR results, we found only a few Shh immunoreactive cells without co-localization of CD31 immunoreactivities (Fig. 3B). We speculate that the Shh-positive cells could be fibroblasts, but its nature awaits further investigation. Ihh or Dhh proteins were not detected in the retinal lesions (data not shown). In the control sham-operated retina, we observed none of the hedgehog family proteins (data not shown). These results suggested that the endothelial cells forming CNV are capable of receiving hedgehog signal by having upregulated signal-transducing components.

Figure 4A shows a representative flat-mount retina stained with anti-CD31 antibody at day 7 after laser delivery. In the control group, CD31-immunoreactive lesions were reproducibly formed in the retina and their size was comparable to those reported previously [1, 14]. We found that the size of neovascularization in the cyclopamine (Shh antagonist)-treated retina was not significantly different from that in the control retina (Fig. 4B), whereas the pur-

morphamine (Shh agonist) treatment significantly increased the size of neovascularization (Fig. 4B).

Sonic hedgehog and its family members are implicated in angiogenesis in various tissues and in various situations including physiological and pathological conditions [12, 39]. Promotion of angiogenesis by Shh has proven effective in wound healing [2] and in preservation of cardiomyocytes in myocardial infarction [30]. Development and maintenance of cancer depends on newly formed blood vessels, and anti-angiogenesis therapies are among the important anti-cancer strategies. Indeed, Shh-targeting therapies are already being applied clinically [35]. As the primary pathogenic phenomenon of AMD is CNV, anti-angiogenesis therapies have been actively developed and brought to clinical use [3, 4, 20]. Shh signaling is thus of interest and its implications in CNV have been demonstrated, that is, that inhibition of Shh signaling by cyclopamine reduced the sizes of laser-induced CNV lesions [42]. Cyclopamine had little effects on the sizes of CNVs in the present study. The discrepancy may be derived from the differences of experimental conditions; Surace *et al.* examined the effects of cyclopamine at 14 days after

laser-induced retinal injury [42], while we focused on earlier time points (at five or seven days after laser irradiation). Based on this assumption, we reproduced the 14-day cyclopamine treatment after laser-induced injury and found that cyclopamine reduced CNV sizes to significantly lower than those in the vehicle control ($p=0.0167<0.05$, $n=8$). Taking these results together, we consider that Shh may not be present at high enough levels to stimulate endothelial cells at relatively early stages after laser-induced injury, because the agonist purmorphamine significantly increased the sizes of CNVs (Fig. 4). We suggest that a possible therapeutic strategy for AMD, especially in early stages, is to prevent Shh upregulation rather than to block Shh signaling. Shh signaling is known to involve crosstalk with other signaling pathways such as TGF- β [7] and FGF [13], and these growth factors upregulate Shh expression [7, 13]. In this regard, blocking these growth factors may be important for the development of new therapies. Another critical point is what kind of cells produce Shh in the injured retina. Although we found no apparent upregulation of Shh protein in the injured retina of early phase, upregulation of Shh by astrocytes in hypoxic conditions has been reported in the brain [16]. Since Müller glia are equivalent to brain astrocytes, inhibition of Müller glial activation is of interest for preventing Shh upregulation.

IV. Acknowledgments

This work was supported in part by the Japan Society for the Promotion of Science (Grant Numbers 26293039 and 15K14354 to AW), and by a research grant from the Takeda Science Foundation to AW. We wish to thank Dr. Ian Smith (Elite Scientific Editing, UK) for assistance in manuscript editing.

V. References

- Ahmad, I., Balasubramanian, S., Del Debbio, C. B., Parameswaran, S., Katz, A. R., Toris, C. and Fariss, R. N. (2011) Regulation of ocular angiogenesis by notch signaling: implications in neovascular age-related macular degeneration. *Invest. Ophthalmol. Vis. Sci.* 52; 2868–2878.
- Asai, J., Takenaka, H., Kusano, K. F., Ii, M., Luedemann, C., Curry, C., Eaton, E., Iwakura, A., Tsutsumi, Y., Hamada, H., Kishimoto, S., Thorne, T., Kishore, R. and Losordo, D. W. (2006) Topical sonic hedgehog gene therapy accelerates wound healing in diabetes by enhancing endothelial progenitor cell-mediated microvascular remodeling. *Circulation* 113; 2413–2424.
- Askou, A. L. (2014) Development of gene therapy for treatment of age-related macular degeneration. *Acta Ophthalmol.* 92 Thesis 3; 1–38.
- Bird, A. C. (2010) Therapeutic targets in age-related macular disease. *J. Clin. Invest.* 120; 3033–3041.
- Camposchiari, P. A., Soloway, P., Ryan, S. J. and Miller, J. W. (1999) The pathogenesis of choroidal neovascularization in patients with age-related macular degeneration. *Mol. Vis.* 5; 34.
- Chakravarthy, U., Evans, J. and Rosenfeld, P. J. (2010) Age related macular degeneration. *Brit. Med. J.* 340; c981.
- Chung, Y. and Fu, E. (2013) Crosstalk between Shh and TGF- β signaling in cyclosporine-enhanced cell proliferation in human gingival fibroblasts. *PLoS One* 8; e70128.
- Cohen, M. M. Jr. (2010) Hedgehog signaling update. *Am. J. Med. Genet. Part A.* 152A; 1875–1914.
- Couch, S. M. and Bakri, S. J. (2011) Review of combination therapies for neovascular age-related macular degeneration. *Semin. Ophthalmol.* 26; 114–120.
- de Jong, P. T. (2006) Age-related macular degeneration. *N. Engl. J. Med.* 355; 1474–1485.
- Dot, C., Parier, V., Behar-Cohen, F., Benezra, D., Jonet, L., Goldenberg, B., Picard, E., Camelo, S., de Kozak, Y., May, F., Soubrane, G. and Jeanny, J. C. (2009) Influence of age on retinochoroidal healing processes after argon photocoagulation in C57bl/6j mice. *Mol. Vis.* 15; 670–684.
- Fuchs, S., Dohle, E. and Kirkpatrick, C. J. (2012) Sonic Hedgehog-mediated synergistic effects guiding angiogenesis and osteogenesis. *Vitam. Horm.* 88; 491–506.
- Fujii, T. and Kuwano, H. (2010) Regulation of the expression balance of angiopoietin-1 and angiopoietin-2 by Shh and FGF-2. *In Vitro Cell. Dev. Biol. Anim.* 46; 487–491.
- Grossniklaus, H. E., Kang, S. J. and Berglin, L. (2010) Animal models of choroidal and retinal neovascularization. *Prog. Retin. Eye Res.* 29; 500–519.
- Haller, J. A. (2013) Current anti-vascular endothelial growth factor dosing regimens: benefits and burden. *Ophthalmology* 120; S3–7.
- He, Q. W., Xia, Y. P., Chen, S. C., Wang, Y., Huang, M., Huang, Y., Li, J. Y., Li, Y. N., Gao, Y., Mao, L., Mei, Y. W. and Hu, B. (2013) Astrocyte-derived sonic hedgehog contributes to angiogenesis in brain microvascular endothelial cells via RhoA/ROCK pathway after oxygen-glucose deprivation. *Mol. Neurobiol.* 47; 976–987.
- Holliday, E. G., Smith, A. V., Cornes, B. K., Buitendijk, G. H. S., Jensen, R. A., Sim, X., Aspelund, T., Aung, T., Baird, P. N., Boerwinkle, E., Cheng, C. Y., van Duijn, C. M., Eiriksdottir, G., Gudnason, V., Harris, T., Hewitt, A. W., Inouye, M., Jonasson, F., Klein, B. E. K., Launer, L., Li, X., Liew, G., Lumley, T., McElduff, P., McKnight, B., Mitchell, P., Psaty, B. M., Rohtchina, E., Rotter, J. I., Scott, R. J., Tay, W., Taylor, K., Teo, Y. Y., Uitterlinden, A. G., Viswanathan, A., Xie, S. C., Wellcome Trust Case Control, C., Vingerling, J. R., Klaver, C. C. W., Tai, E. S., Siscovick, D., Klein, R., Cotch, M. F., Wong, T. Y., Attia, J., Wang, J. J. and Consortium, W. T. C. C. (2013) Insights into the genetic architecture of early stage age-related macular degeneration: a genome-wide association study meta-analysis. *PLoS One* 8; e53830.
- Huang, H., Shen, J. and Viores, S. A. (2011) Blockade of VEGFR1 and 2 suppresses pathological angiogenesis and vascular leakage in the eye. *PLoS One* 6; e21411.
- Hui, C.-C. and Angers, S. (2011) Gli proteins in development and disease. *Annu. Rev. Cell Dev. Biol.* 27; 513–537.
- Izumi-Nagai, K., Nagai, N., Ohgami, K., Satofuka, S., Ozawa, Y., Tsubota, K., Ohno, S., Oike, Y. and Ishida, S. (2008) Inhibition of choroidal neovascularization with an anti-inflammatory carotenoid astaxanthin. *Invest. Ophthalmol. Vis. Sci.* 49; 1679–1685.
- Izzi, L., Lévesque, M., Morin, S., Laniel, D., Wilkes, B. C., Mille, F., Krauss, R. S., McMahon, A. P., Allen, B. L. and Charron, F. (2011) Boc and Gas1 each form distinct Shh receptor complexes with Ptch1 and are required for Shh-mediated cell proliferation. *Dev. Cell.* 20; 788–801.
- Jager, R. D., Mieler, W. F. and Miller, J. W. (2008) Age-related macular degeneration. *N. Engl. J. Med.* 358; 2606–2617.
- Jian, L., Panpan, Y. and Wen, X. (2013) Current choroidal neovascularization treatment. *Ophthalmologica* 230; 55–61.

24. Kang, J.-S., Zhang, W. and Krauss, R. S. (2007) Hedgehog signaling: cooking with Gas1. *Sci. STKE*. 2007; pe50.
25. Kang, S., Roh, Y.-J. and Kim, I.-B. (2013) Antiangiogenic effects of tozozanib, an oral VEGF receptor tyrosine kinase inhibitor, on experimental choroidal neovascularization in mice. *Exp. Eye Res.* 112; 125–133.
26. Katoh, M. (2013) Therapeutics targeting angiogenesis: Genetics and epigenetics, extracellular miRNAs and signaling networks (Review). *Int. J. Mol. Med.* 32; 763–767.
27. Kavran, J. M., Ward, M. D., Oladosu, O. O., Mulepati, S. and Leahy, D. J. (2010) All mammalian Hedgehog proteins interact with cell adhesion molecule, down-regulated by oncogenes (CDO) and brother of CDO (BOC) in a conserved manner. *J. Biol. Chem.* 285; 24584–24590.
28. Khandhadia, S., Cipriani, V., Yates, J. R. W. and Lotery, A. J. (2012) Age-related macular degeneration and the complement system. *Immunobiology* 217; 127–146.
29. Lee, E. and Rewolinski, D. (2010) Evaluation of CXCR4 inhibition in the prevention and intervention model of laser-induced choroidal neovascularization. *Invest. Ophthalmol. Vis. Sci.* 51; 3666–3672.
30. Mackie, A. R., Klyachko, E., Thorne, T., Schultz, K. M., Millay, M., Ito, A., Kamide, C. E., Liu, T., Gupta, R., Sahoo, S., Misener, S., Kishore, R. and Losordo, D. W. (2012) Sonic hedgehog-modified human CD34+ cells preserve cardiac function after acute myocardial infarction. *Circ. Res.* 111; 312–321.
31. Martinelli, D. C. and Fan, C.-M. (2007) Gas1 extends the range of Hedgehog action by facilitating its signaling. *Genes Dev.* 21; 1231–1243.
32. Morita, S., Furube, E., Mannari, T., Okuda, H., Tatsumi, K., Wanaka, A. and Miyata, S. (2015) Vascular endothelial growth factor-dependent angiogenesis and dynamic vascular plasticity in the sensory circumventricular organs of adult mouse brain. *Cell Tissue Res.* 359; 865–884.
33. Nagase, M., Nagase, T., Koshima, I. and Fujita, T. (2006) Critical time window of hedgehog-dependent angiogenesis in murine yolk sac. *Microvasc. Res.* 71; 85–90.
34. Nagase, T., Nagase, M., Yoshimura, K., Fujita, T. and Koshima, I. (2005) Angiogenesis within the developing mouse neural tube is dependent on sonic hedgehog signaling: possible roles of motor neurons. *Genes Cells* 10; 595–604.
35. Newton, H. B. (2004) Molecular neuro-oncology and development of targeted therapeutic strategies for brain tumors. Part 2: PI3K/Akt/PTEN, mTOR, SHH/PTCH and angiogenesis. *Expert Rev. Anticancer Ther.* 4; 105–128.
36. Okada, A., Charron, F., Morin, S., Shin, D. S., Wong, K., Fabre, P. J., Tessier-Lavigne, M. and McConnell, S. K. (2006) Boc is a receptor for sonic hedgehog in the guidance of commissural axons. *Nature* 444; 369–373.
37. Olsen, C. L., Hsu, P.-P. P., Glienke, J., Rubanyi, G. M. and Brooks, A. R. (2004) Hedgehog-interacting protein is highly expressed in endothelial cells but down-regulated during angiogenesis and in several human tumors. *BMC Cancer* 4; 43.
38. Pola, R., Ling, L. E., Silver, M., Corbley, M. J., Kearney, M., Blake Pepinsky, R., Shapiro, R., Taylor, F. R., Baker, D. P., Asahara, T. and Isner, J. M. (2001) The morphogen Sonic hedgehog is an indirect angiogenic agent upregulating two families of angiogenic growth factors. *Nat. Med.* 7; 706–711.
39. Renault, M. A., Roncalli, J., Tongers, J., Thorne, T., Klyachko, E., Misener, S., Volpert, O. V., Mehta, S., Burg, A., Luedemann, C., Qin, G., Kishore, R. and Losordo, D. W. (2010) Sonic hedgehog induces angiogenesis via Rho kinase-dependent signaling in endothelial cells. *J. Mol. Cell. Cardiol.* 49; 490–498.
40. Sengupta, N., Afzal, A., Caballero, S., Chang, K.-H., Shaw, L. C., Pang, J.-J., Bond, V. C., Bhutto, I., Baba, T., Luty, G. A. and Grant, M. B. (2010) Paracrine modulation of CXCR4 by IGF-1 and VEGF: implications for choroidal neovascularization. *Invest. Ophthalmol. Vis. Sci.* 51; 2697–2704.
41. Sheridan, C. M., Pate, S., Hiscott, P., Wong, D., Pattwell, D. M. and Kent, D. (2009) Expression of hypoxia-inducible factor-1alpha and -2alpha in human choroidal neovascular membranes. *Graefes Arch. Clin. Exp. Ophthalmol.* 247; 1361–1367.
42. Surace, E. M., Balaggon, K. S., Tessitore, A., Mussolino, C., Cotugno, G., Bonetti, C., Vitale, A., Ali, R. R. and Auricchio, A. (2006) Inhibition of ocular neovascularization by hedgehog blockade. *Mol. Ther.* 13; 573–579.
43. Tatsumi, K., Takebayashi, H., Manabe, T., Tanaka, K. F., Makinodan, M., Yamauchi, T., Makinodan, E., Matsuyoshi, H., Okuda, H., Ikenaka, K. and Wanaka, A. (2008) Genetic fate mapping of Olig2 progenitors in the injured adult cerebral cortex reveals preferential differentiation into astrocytes. *J. Neurosci. Res.* 86; 3494–3502.
44. van Lookeren Campagne, M., LeCouter, J., Yaspan, B. L. and Ye, W. (2014) Mechanisms of age-related macular degeneration and therapeutic opportunities. *J. Pathol.* 232; 151–164.
45. Yang, X.-M., Wang, Y.-S., Zhang, J., Li, Y., Xu, J.-F., Zhu, J., Zhao, W., Chu, D.-K. and Wiedemann, P. (2009) Role of PI3K/Akt and MEK/ERK in mediating hypoxia-induced expression of HIF-1alpha and VEGF in laser-induced rat choroidal neovascularization. *Invest. Ophthalmol. Vis. Sci.* 50; 1873–1879.
46. Zampros, I., Praidou, A., Brazitikos, P., Ekonomidis, P. and Androudi, S. (2012) Antivascular endothelial growth factor agents for neovascular age-related macular degeneration. *J. Ophthalmol.* 2012; 319728.
47. Zhou, T., Hu, Y., Chen, Y., Zhou, K. K., Zhang, B., Gao, G. and Ma, J. X. (2010) The pathogenic role of the canonical Wnt pathway in age-related macular degeneration. *Invest. Ophthalmol. Vis. Sci.* 51; 4371–4379.